The Astrophysical Journal, 576:120–134, 2002 September 1


# ORPHAN AFTERGLOWS OF COLLIMATED GAMMA-RAY BURSTS: RATE PREDICTIONS AND PROSPECTS FOR DETECTION

Tomonori Totani[1] and Alin Panaitescu
Princeton University Observatory, Peyton Hall, Princeton, NJ 08544-1001
*Received 2002 April 5; accepted 2002 May 10*

## ABSTRACT

We make a quantitative prediction for the detection rate of orphan gamma-ray burst (GRB) afterglows as a function of flux sensitivity in X-ray, optical, and radio wave bands, based on a recent model of collimated GRB afterglows. We find that the orphan afterglow rate strongly depends on the opening angle of the jet (roughly $\propto\theta_{\rm jet}^{-2}$), as expected from simple geometrical consideration, if the total jet energy is kept constant as suggested by recent studies. The relative beaming factor $b_{\rm rel}$, i.e., the ratio of all afterglow rates including orphans to those associated with observable prompt GRBs, could be as high as $b_{\rm rel}\gtrsim 100$ for searches deeper than $R\sim 24$, depending on afterglow parameters. To make the most plausible predictions, we average the model emission for 10 sets of afterglow parameters obtained through fits to 10 well-observed, collimated GRB jets, weighted by the sky coverage of each jet. Our model expectations are consistent with the results (or constraints) obtained by all past searches. We estimate the number of orphan afterglows in the first 1500 deg$^2$ field of the Sloan Digital Sky Survey (SDSS) to be about 0.2. The relative beaming factor $b_{\rm rel}$ is rapidly increasing with the search sensitivity: $b_{\rm rel}\sim 3$ for the SDSS sensitivity to transient objects in the northern sky ($R\sim 19$), $\sim$14 for the past high-$z$ supernova searches ($R\sim 23$), and $\sim$50 for the sensitivity of the Subaru Suprime-Cam ($R\sim 26$). Predictions are made for the current facilities and future projects in X-ray, optical, and radio bands. Among them, the southern sky observation of the SDSS (sensitive to transients down to $R\sim 23$) could detect $\sim$40 orphan afterglows during the 5 yr operation. The Allen Telescope Array would find about 200 afterglows in a radio band at $\sim$0.1–1 mJy with $b_{\rm rel}\sim 15$.

*Subject headings:* gamma rays: bursts — ISM: jets and outflows — surveys

## 1. INTRODUCTION

Gamma-ray bursts (GRBs) are now confirmed to be located at cosmological distances, and they are recognized as the most energetic explosion in the universe in terms of isotropic equivalent luminosity, while their origin still remains a mystery. The redshift of GRB 990123 was $z=1.6$, and its total energy emitted as gamma rays, estimated by its energy flux and redshift, is $E\sim 3\times 10^{54}$ ergs assuming isotropic radiation (Kulkarni et al. 1999). This energy is equivalent to a rest-mass energy of 1.7 $M_\odot c^2$, and it is almost impossible to explain by explosions of objects with stellar mass scale. This is why most researchers in this field now consider GRBs to likely be strongly collimated, with a typical collimation factor of $4\pi/\Delta\Omega\gtrsim 100$. It is then important to test this hypothesis by observations for better understanding of the nature of GRBs.

A direct consequence for such GRB collimation is that the rate of GRB afterglows may be much higher than those associated with observable prompt GRBs. GRBs are believed to be produced by dissipation of kinetic energy of ultrarelativistic outflow from the central engine with a Lorentz factor of $\Gamma\sim 100$–1000. The outflow is eventually decelerated by interaction with interstellar matter, just like supernova remnants, to produce radiation called afterglows. After $\Gamma$ decreases to $\Gamma\sim\theta_{\rm jet}^{-1}$, where $\theta_{\rm jet}$ is the opening angle of the jet, the beaming of radiation is wider than that of outflow; thus, the afterglow becomes observable from directions different from that of the original gamma radiation. At the same time, the sideways expansion increases the opening angle of the jet from the original angle of $\theta_{\rm jet}$.

Therefore, a serendipitous search of GRB afterglows without prompt GRBs is an important test for the beaming of GRBs (Rhoads 1997). Several efforts have been made in various wave bands. Past X-ray surveys set a constraint of $b_{\rm rel}\lesssim$ several (Grindlay 1999; Greiner et al. 2000), where $b_{\rm rel}$ is the "relative" beaming factor, i.e., the ratio of all afterglow rates including orphans to the rate of those with on-axis GRBs.[2] Perna & Loeb (1998) set a crude upper limit of $b_{\rm rel}\lesssim 1.5\times 10^3$ by radio source counts. Schaefer (2002) searched a 264 deg$^2$ field down to $R\sim 21$, but no afterglow candidate was found. The past survey for high-redshift supernovae should also give some constraint on the orphan GRB afterglow rate (see, e.g., Rees 1999). Recently, Vanden Berk et al. (2002) reported a possible orphan afterglow found in the initial 1500 deg$^2$ data of the Sloan Digital Sky Survey (SDSS). However, Gal-Yam et al. (2002) reported that the host galaxy of the SDSS transient is a highly variable, radio-loud active galactic nucleus (AGN), and hence it was almost certainly not related to a GRB.

The interpretation of these results is, however, not straightforward. They must be compared with a realistic theoretical prediction of $b_{\rm rel}$, which is generally dependent

[1] Theory Division, National Astronomical Observatory, Mitaka, Tokyo 181-8588, Japan.

[2] We used the term "relative" since $b_{\rm rel}$ reflects the relative beaming of radiation between prompt GRBs and typical afterglows detectable in an orphan afterglow search.

on the wave band and sensitivity of surveys. Recently, Dalal, Griest, & Pruet (2002) argued, based on a simple analytical investigation, that the value of $b_{\rm rel}$ is not sufficiently large for the sensitivity that can be achieved by the current facilities, even if GRBs are strongly collimated. They also argued that the rate of orphan afterglows is insensitive to the jet opening angle, and hence they concluded that the orphan afterglow search hardly constrains the GRB collimation in practice. What makes the situation even more complicated is the possibility that orphan afterglows can be produced by processes other than the collimation; for example, a "failed" GRB or a "dirty fireball" may produce afterglows at longer wavelength while there is no prompt gamma-ray emission (Huang, Dai, & Lu 2002).

In this paper we present a realistic prediction of orphan afterglow rate as a function of search sensitivity in various wave bands, based on a popular afterglow model of collimated GRBs that has been tested against a number of afterglow observations. We find that the orphan afterglow rate rapidly increases with GRB jet collimation roughly as $b_{\rm rel} \propto \theta_{\rm jet}^{-2}$, if GRB jets have roughly constant energies against various $\theta_{\rm jet}$, as suggested by recent studies (Frail et al. 2001; Panaitescu & Kumar 2001). Therefore, the orphan afterglow search could still be a powerful tool to get information on collimation of GRB jets. Even if the theoretical prediction is also affected by other possible components of ejecta from successful or failed GRBs with a lower Lorentz factor, it would be useful to make a prediction for the abundance of orphan afterglows by the "nominal" (i.e., without any other hypothetical components) jet model of GRB afterglows as realistic as possible since the jet model is a relatively reliable method of transforming the on-axis light curves to off-axis ones compared to other theoretical possibilities of orphan afterglows. It can be used as a baseline prediction when one interprets the results of past and future searches for faint extragalactic transient objects.

To make plausible predictions, we take the observed radio, optical, and X-ray emission of 10 GRB afterglows with a wide variety of estimated jet opening angles—GRBs 970508, 980519, 990123, 990510, 991208, 991216, 000301c, 000418, 000926, and 010222—and calculate their emission as it would be seen at various angles relative to the jet axis. This is done within the framework of collimated jets decelerated by the circumburst medium (Mészáros & Rees 1997) and undergoing lateral expansion (Rhoads 1999), using the treatment presented by Panaitescu & Kumar (2000) and Kumar & Panaitescu (2000). With the aid of this model, Panaitescu & Kumar (2002) have determined the physical parameters of the 10 afterglows by modeling their broadband emission. We employ these 10 sets of jet parameters to calculate their emission for any off-axis observer location. The detection rate as a function of the X-ray/optical/radio search sensitivity is further obtained by integrating over the viewing angle and the GRB rate history in the universe.

The paper will be organized as follows: Section 2 reviews the model of collimated afterglows used here, and some discussions are presented on the physics of collimated afterglows concerning the detectability of orphan afterglows. Section 3 is for the formulation of orphan afterglow rate calculation. The results are presented in § 4; they are compared with various past search results, and predictions for the current and future facilities are made in § 5. Discussions are given in § 6, including comparison with previous studies, another possible picture of GRB jets, and caveats of our predictions. Our main conclusions are presented in § 7.

## 2. THE AFTERGLOW MODEL OF COLLIMATED GRBs

The dynamics of a GRB jet is calculated by tracking its total energy (allowing for radiative losses) and mass. The jet spreads laterally at the sound speed, and it is assumed to be uniform within its aperture (i.e., the same energy per solid angle in any direction) and have sharp boundaries. The afterglow synchrotron emission and the radiative losses are calculated from the strength of the magnetic field in the shocked gas and the power-law distribution of shock-accelerated electrons, taking into account their radiative (synchrotron and inverse Compton) cooling. To obtain observer light curves, the jet emission is integrated over its surface, allowing for the differential relativistic beaming and the spread in the photon arrival time across the jet surface.

The afterglow jet model has three parameters that determine the jet dynamics (the initial jet energy $E_{\rm jet}$, initial jet half-angle $\theta_{\rm jet}$, and external particle density $n_{\rm ext}$) and three parameters pertaining to the microphysics of shocks (the fraction of the postshock energy density in magnetic fields $\epsilon_B$, the fractional energy of the least energetic injected electrons $\epsilon_e$, and the power-law index $p$ of the shock-accelerated electron energy distribution). For hard electron distributions with $p < 2$, two other parameters become relevant: the total fraction of the internal energy of the shocked fluid imparted to electrons, which sets a "cutoff" of the electron distribution at high electron energies, and the larger (than 2) power-law index of the electron index above the cutoff. The passage of the spectral break associated with the electron distribution cutoff through the optical domain may yield a light-curve break, as suggested by the sharp break seen in GRB 000301c and the steep decay of the optical emission of GRB 991208.

Figures 1, 2, and 3 show the X-ray, optical, and radio afterglow light curves, respectively, for the above 10 jets as they would be seen from various viewing angles relative to the center of the jet $\theta_{\rm obs}$. It can be seen that the behavior of off-axis light curves is very different for different sets of model parameters, even when the opening angle of the jet $\theta_{\rm jet}$ is similar. As illustrated in Figure 2, the "best case," i.e., the highest rate for orphan afterglow searches, is expected for GRB 991216 ($\theta_{\rm jet} = 2.^\circ7$), whose peak of optical light curves is at $R \sim 24$ (when it is placed at $z = 1$) for an observer located with an angle $\theta_{\rm obs} = 30^\circ$. If one searches orphan afterglows with a sensitivity better than this, one could find them at a rate more than 100 times higher than that expected from spherical GRBs (i.e., $b_{\rm rel} > 100$). The other extreme is the cases of GRB 980519 or GRB 990123. Even though their jet opening angle $\theta_{\rm jet}$ is not much different from that of GRB 991216, the peaks of optical light curves are difficult to detect when an observer is located at $\theta_{\rm obs} \gtrsim 10^\circ$. In these cases the relative beaming factor is at most $b_{\rm rel} \lesssim 10$.

The dependence of $b_{\rm rel}$ on the jet initial opening (and other jet properties), as well as the reason for which $b_{\rm rel}$ is maximal for the 991216 afterglow, can be obtained using a simplified model where all the afterglow emission originates from a single point on the jet axis (Dalal et al. 2002; Granot et al. 2002) whose dynamics is that of an expanding jet (Rhoads 1999). For narrow ($\theta_{\rm jet} \ll 1$ rad), relativistic jets and a homogeneous medium, it can be shown that the jet

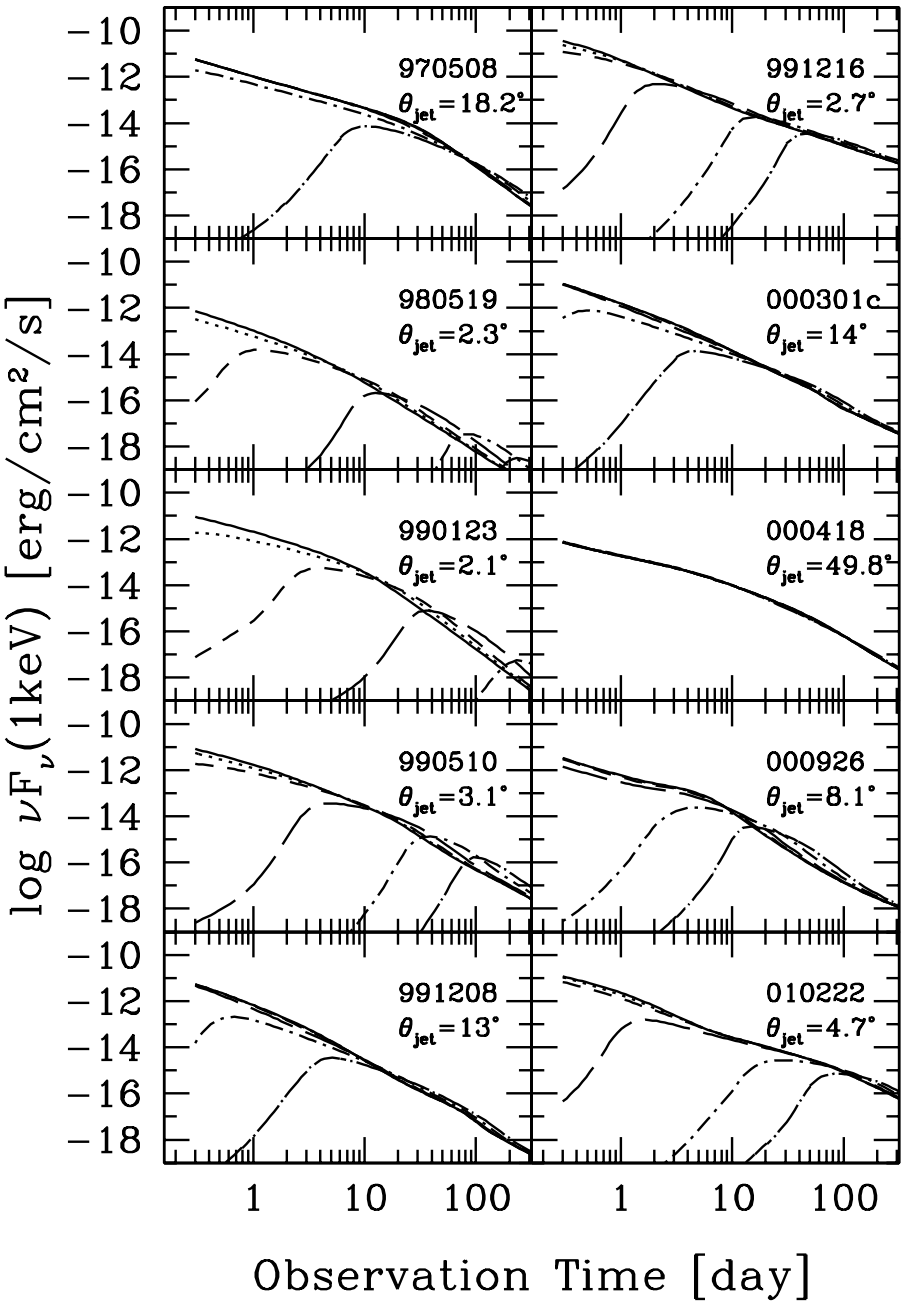


FIG. 1.—Light curves of off-axis GRB afterglows in the X-ray band (1 keV) for the 10 well-observed GRBs (name and the opening angle of the jet indicated in each panel). Note that the distance is assumed to be $z = 1$ for all GRBs, for comparison. The light curves are shown for different viewing angles from the center of the jet, as $\theta_{\rm obs} = 1^\circ$, $3^\circ$, $5^\circ$, $10^\circ$, $20^\circ$, and $30^\circ$ for the solid, dotted, short-dashed, long-dashed, short-dash–dotted, and long-dash–dotted lines, respectively.

Lorentz factor $\gamma$ is

$$\gamma(t_0) = \theta_{\rm jet}^{-1}\left(\frac{t_0}{t_{j,0}}\right)^{-n}, \quad n = \begin{cases} \frac{3}{8}, & t_0 < t_{j,0}\,, \\ \frac{1}{2}, & t_0 > t_{j,0}\,, \end{cases} \tag{1}$$

where the subscript "0" indicates the time (since the prompt gamma-ray emission) measured by an on-axis observer ($\theta_{\rm obs} = 0$), $t_{j,0}$ being the "jet-break time," i.e., the time when $\gamma = \theta_{\rm jet}^{-1}$ and the on-axis observer "sees" the entire jet surface and a break in the light curve. Taking into account that the photon arrival time for an arbitrary observer location $\theta_{\rm obs}$ is given by $dt/dt_0 = 2\gamma^2(1 - \beta\cos\theta_{\rm obs})$, $\beta$ being the jet speed in units of the speed of light, equation (1) gives the jet Lorentz factor as a function of the time $t$ when photons arrive at $\theta_{\rm obs}$:

$$\frac{\gamma(t)}{f^n(\gamma)} = \frac{\theta_{\rm jet}^{-1}}{f^n(\theta_{\rm jet}^{-1})}\left[\frac{t}{t_j(\theta_{\rm obs})}\right]^{-n}, \tag{2}$$

where

$$f(\gamma) \equiv \cos\theta_{\rm obs} + 8[2 - \ln(\min\{1,\, \gamma\theta_{\rm jet}\})]\gamma^2 \sin^2\left(\frac{\theta_{\rm obs}}{2}\right). \tag{3}$$

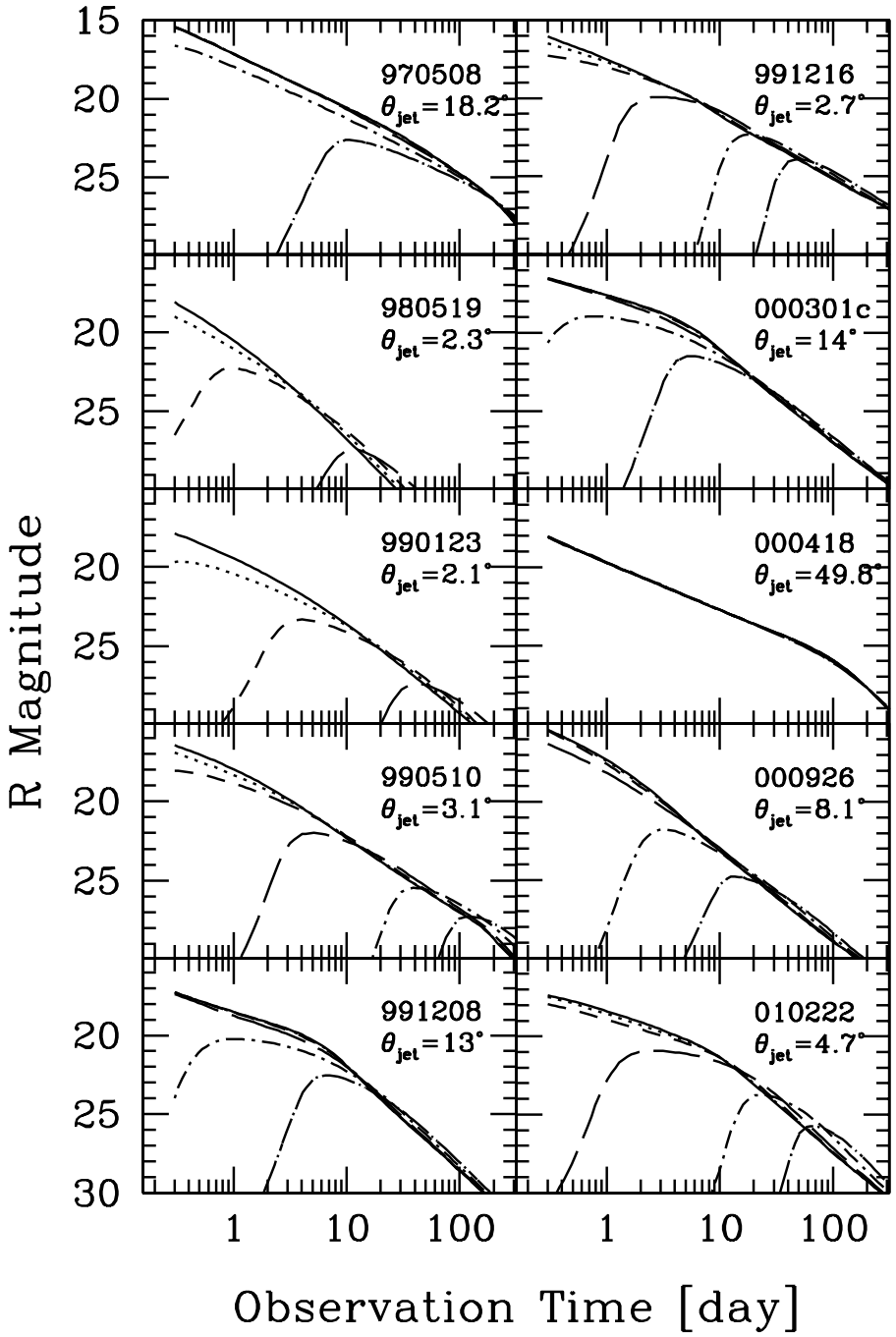


FIG. 2.—Same as Fig. 1, but for the optical ($R$) band

The above $f(\gamma)$ relates the photon arrival time at $\theta_{\rm obs}$ to that for an on-axis observer: $t = f(\gamma)t_0$; therefore, in equation (2), $t_j(\theta_{\rm obs}) = f(\theta_{\rm jet}^{-1})t_{j,0}$. For an observer located well outside the jet opening ($\theta_{\rm obs} \gg \theta_{\rm jet}$), the received jet emission is Doppler boosted in frequency by the same factor $\mathscr{D} = [\gamma(1 - \beta\cos\theta_{\rm obs})]^{-1}$, its intensity being relativistically enhanced by $\mathscr{D}^3$. Thus, the received afterglow flux $F(\nu, t)$ at $\theta_{\rm obs}$ is related to that seen by an on-axis observer, $F_0(\nu, t_0)$, through

$$F(\nu, t) = g^{-3}(\gamma)F_0\left(g\nu, \frac{t}{f}\right), \qquad (4)$$

where

$$g(\gamma) \equiv \cos\theta_{\rm obs} + 4\gamma^2 \sin^2\left(\frac{\theta_{\rm obs}}{2}\right). \qquad (5)$$

The observed GRB afterglows have power-law optical spectra and light curves: $F_0(\nu, t_0) \propto \nu^{-\delta} t_0^{-\alpha}$ (for the above-mentioned 10 afterglows, $\delta \in [0.6, 1.5]$, $\alpha \equiv \alpha_1 \in [0.7, 1.7]$ at $t_0 < t_{j,0}$, and $\alpha \equiv \alpha_2 \in [1.6, 3.0]$ at $t_0 > t_{j,0}$). Therefore, equation (4) leads to

$$F(\nu, t) \propto f^{\alpha}(\gamma)[g(\gamma)]^{-(3+\delta)} t^{-\alpha}, \qquad (6)$$

with $\gamma(t)$ given by equation (2).

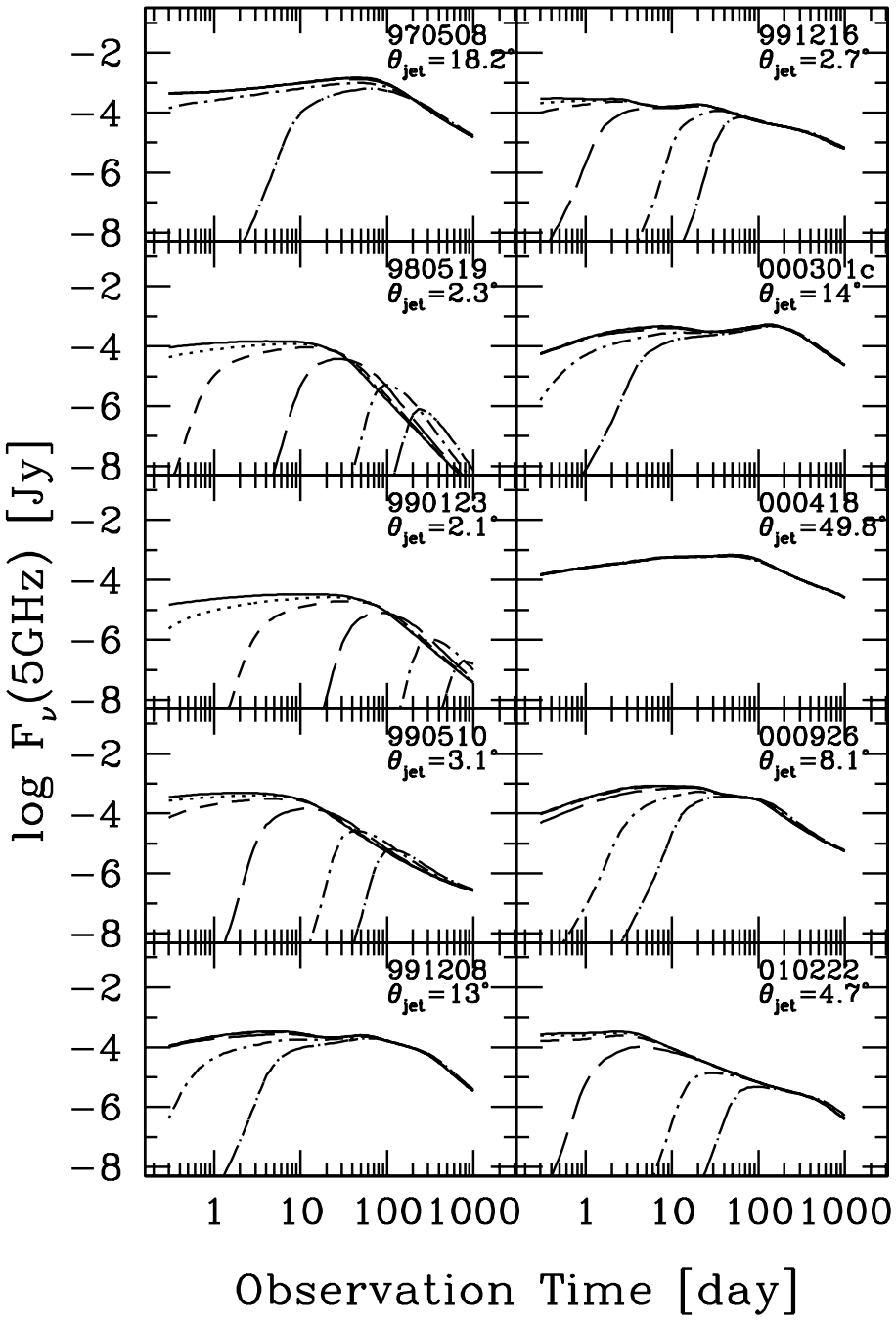


FIG. 3.—Same as Fig. 1, but for the radio (5 GHz) band

For $t < t_j$, when $\gamma\theta_{\rm jet} > 1$, the above equations yield $\gamma \propto t^{-3/2}$ and $F(\nu, t) \propto \gamma^{2(\alpha_1-\delta-3)}t^{-\alpha_1} \propto t^{3(3+\delta)-4\alpha_1}$ in the $\theta_{\rm obs} \ll 1$ limit, i.e., a light curve with a sharp rise. At $t > t_j$ and before the time $t_p$ when $\gamma(t_p) = \theta_{\rm obs}^{-1}$, $\gamma \propto \exp\{-2t/t_j\}$ and $F(\nu, t) \propto \exp\{4(3 + \delta - \alpha_2)(t/t_j)\}$; thus, the light curve continues to rise. At $t > t_p$ the $f$ and $g$ functions asymptotically approach unity, so that the evolution of the jet Lorentz factor and the afterglow light curves become those for an on-axis observer: $\gamma \propto t^{-1/2}$ and $F(\nu, t) \propto t^{-\alpha_2}$, respectively. Therefore, the afterglow light curve for $\theta_{\rm obs}$ peaks around the time $t_p$ when $\gamma(t_p)\theta_{\rm obs} = 1$. Taking into account that $t_p = f[\gamma(t_p)]t_{p,0}$, where $t_{p,0} \simeq (\theta_{\rm obs}/\theta_{\rm jet})^2 t_{j,0}$ (from eq. [1]) is the corresponding photon arrival time for an on-axis observer and $f(\theta_{\rm obs}^{-1}) \simeq 5 + 2\ln(\theta_{\rm obs}/\theta_{\rm jet})$ in the $\theta_{\rm obs} \ll 1$ limit, it follows that the afterglow light curve seen by an observer at $\theta_{\rm obs}$ peaks at

$$t_p = \left(5 + 2\ln\frac{\theta_{\rm obs}}{\theta_{\rm jet}}\right)\left(\frac{\theta_{\rm obs}}{\theta_{\rm jet}}\right)^2 t_{j,0} \ . \qquad (7)$$

In the same $\theta_{\rm obs} \ll 1$ limit, $g[\gamma(t_p)] \simeq 2$; therefore, equations (4) and (7) give, for the peak flux,

$$F(\nu, t_p) = 2^{-(3+\delta)}\left(\frac{\theta_{\rm obs}}{\theta_{\rm jet}}\right)^{-2\alpha_2} F_0(\nu, t_{j,0}) \ . \qquad (8)$$

It may not be easy to infer $t_p$ for an observed orphan afterglow since we do not know the precise time of the prompt burst time. However, if there are enough data points to construct a light curve, it may be possible to infer $t_p$ only from orphan afterglows. Then, together with an empirical relation between the jet-break time $t_{j,0}$ and flux $F_0(\nu, t_{j,0})$, calibrated with the afterglows that were seen on-axis (i.e., preceded by a GRB), equations (7) and (8) can be used to determine the relative observer location $\theta_{\rm obs}/\theta_{\rm jet}$, $t_{j,0}$, and $F_0(\nu, t_{j,0})$ from the inferred peak time $t_p$ and observed flux $F(\nu, t_p)$ of an orphan GRB afterglow.

From equation (8) it follows that only jets seen at an angle less than

$$\theta_{\rm max} = \left[2^{-(3+\delta)} \frac{F_0(\nu, t_{j,0})}{F_{\rm lim}}\right]^{1/(2\alpha_2)} \theta_{\rm jet} \qquad (9)$$

can be detected above a given detection threshold $F_{\rm lim}$. Therefore, the relative beaming factor is $b_{\rm rel} = (\theta_{\rm max}/\theta_{\rm jet})^2 \propto [2^{-\delta} F_0(\nu, t_{j,0})]^{1/\alpha_2}$. The $b_{\rm rel}$ that can be inferred for each afterglow shown in Figure 2, for a given threshold, is consistent with this estimation of $b_{\rm rel}$. Among the set of 10 afterglows, GRB 991216 has one of the largest jet-break fluxes $F_0(\nu, t_{j,0})$ (note that for this afterglow, $t_{j,0} \lesssim 1$ day, the sharper break seen in Fig. 2 at several days being due to the passage through the optical band of a spectral break), hardest optical spectra, and shallowest decays after the jet-break time. For these reasons, its $b_{\rm rel}$ is the largest in our sample of afterglows, and GRB 991216 dominates the detection probability of orphan afterglows.

## 3. FORMULATIONS FOR THE RATE CALCULATION

First we calculate the expected number of orphan afterglows per unit solid angle $N_{\rm exp}(F_{\rm lim})$, which can be detected by a snapshot observation with a given sensitivity $F_{\rm lim}$. This quantity directly provides the detectability of afterglows in a search in which transient objects are found by comparison of several snapshot images taken at time intervals longer than the duration $T$ over which the afterglow is brighter than the sensitivity. On the other hand, the detection rate in a survey of consecutive monitoring with a timescale longer than $T$ can be estimated by $R_{\rm exp} \sim N_{\rm exp}/T$ per unit solid angle and observation time.

The afterglow flux at any frequency and observer's time viewed by an observer with arbitrary $\theta_{\rm obs}$ is calculated with the model presented in the previous section. From there we can calculate the time duration for an observer, $T(x, z, \theta_{\rm obs}, F_{\rm lim})$, during which an afterglow is brighter than a given sensitivity, where $z$ is redshift and $x$ symbolically represents a specific type of GRB afterglow. Then, the expected number $N_{\rm exp}$ per all sky can be written as

$$N_{\rm exp}(F_{\rm lim}) = \int dx \int dz \int_0^\pi d\theta_{\rm obs} \frac{\sin\theta_{\rm obs}}{2} \times \frac{dV}{dz} \frac{R_{\rm GRB}(x, z)}{1+z} T(x, z, \theta_{\rm obs}, F_{\rm lim}) , \qquad (10)$$

where $(dV/dz)$ is the standard comoving volume element in all sky and $R_{\rm GRB}(x, z)$ is the comoving GRB rate density of type $x$. It should be noted that $R_{\rm GRB}$ is the true rate of GRBs including unobservable ones whose jets are not directed to us.

As shown in the previous section, the detectability of orphan afterglows sensitively depends on afterglow parameters. In order to take this into account and make the most plausible prediction in an empirical way, we replace the integration over $x$ by the sum of the 10 well-observed afterglows presented in the previous section. We assume that all the population of observable GRBs is represented by those 10 bursts with an equal weight and that it is independent of redshift. If detection of GRBs is flux limited, then a simple sum of the 10 observed bursts having very different gamma-ray luminosities might induce some bias from the true population. However, GRBs are generally bright enough to be detected even at very large cosmological distances, and hence the effect of the flux limit is expected to be insignificant. In addition, the redshifts of the 10 GRBs are in a rather small range. Therefore, we expect that the above treatment is not unreasonable. On the other hand, it should be noted that we must take into account the estimated opening angle of jets; the GRB rate inferred from the observed number of GRBs assuming isotropic emission ($R_{\rm iso}$) is not the true GRB rate, but it should be multiplied by the inverse of sky coverage of gamma-ray emission, $2/(1-\cos\theta_{\rm jet})$, to obtain $R_{\rm GRB}$.[3] Then, the integration over $x$ in equation (10) should be replaced by the sum of $N_{\rm GRB}$ (=10) GRBs as

$$N_{\rm exp}(F_{\rm lim}) = \sum_{i=1}^{N_{\rm GRB}} \frac{1}{N_{\rm GRB}} \int dz \int_0^\pi d\theta_{\rm obs} \frac{\sin\theta_{\rm obs}}{2} \frac{dV}{dz} \frac{R_{\rm iso}(z)}{1+z} \times \left(\frac{1-\cos\theta_{{\rm jet},i}}{2}\right)^{-1} T(i, z, \theta_{\rm obs}, F_{\rm lim}) . \qquad (11)$$

It should be noted that the 10 GRBs chosen by Panaitescu & Kumar (2002) are well observed, with good temporal coverage at various frequencies, and show a light-curve break. This suggests that there may be a systematic bias toward strongly collimated GRBs in our selection. We note that the 10 GRB afterglows used here represent about $\frac{1}{3}$ of all bursts for which optical afterglows were found. This indicates that the formulation above overestimates by a factor of up to 3 the real orphan afterglow rate if the other $\frac{2}{3}$ GRB afterglows are isotropic and hardly contribute to $N_{\rm exp}$. This is probably not much larger than other model uncertainties. Therefore, we believe that the 10 GRBs represent the whole GRB population reasonably well.

We assume that $R_{\rm iso}(z)$ traces the cosmic star formation history (Totani 1997; Wijers et al. 1998). Based on the recent observational estimates (see, e.g., Totani & Takeuchi 2002 for a summary of recent studies on this issue), we assume that $R_{\rm iso}(z) \propto (1+z)^{3.77}$ at $0 < z < 1$ and that $R_{\rm iso}(z)$ is constant at $z > 1$, when the Einstein–de Sitter universe is adopted. We set an upper cutoff for redshift as $z_u = 5$. The normalization of this rate density is fixed at $z = 0$, as $R_{\rm iso}(0) = 2 \times 10^{-10} (h/0.7)^3$ yr$^{-1}$ Mpc$^{-3}$, where $h = H_0/(100$ km s$^{-1}$ Mpc$^{-1})$, based on the fitting to the observed flux distribution (i.e., the $\log N$–$\log P$ relation) of the BATSE GRBs (Totani 1999; Schmidt 1999). Throughout this paper we adopt a standard $\Lambda$-dominated universe with $(h, \Omega_0, \Omega_\Lambda) = (0.7, 0.3, 0.7)$, and the cosmology dependence of $R_{\rm iso}(z)$ is corrected appropriately.

[3] Here, we have assumed that the opening angle of gamma-ray emission is the same with that of the jet inferred from the afterglow fitting, but this is not necessarily true. We will discuss this point later in § 6.3.

## 4. RESULTS

Figures 4, 5, and 6 show the result of calculation for $N_{\rm exp}$ as a function of sensitivity in X-ray (1 keV), optical ($R$), and radio (5 GHz) wave bands, respectively. We also show the rate expected only from on-axis afterglows, i.e., associated with prompt GRBs. This rate, $N_{\rm on}$, is obtained by replacing the range of integration over $\theta_{\rm obs} = 0 - \pi$ by $\theta_{\rm obs} = 0 - \theta_{\rm jet}$ in equation (11). The relative beaming factor, $b_{\rm rel} \equiv N_{\rm exp}/N_{\rm on}$, is shown in the lower panel. The mean values of redshift and $T$ are also shown; here we calculated the average of $\log z$ and $\log T$ because of considerable scatter of these values at a fixed sensitivity. We also give another mean time,

$$\left\langle \frac{1}{T} \right\rangle^{-1} \equiv \left( \frac{\int dN_{\rm exp}/T}{N_{\rm exp}} \right)^{-1}, \qquad (12)$$

where integration with $dN_{\rm exp}$ represents that of equation (11). We give this quantity because we can translate $N_{\rm exp}$ into detection rate per time in a consecutive monitoring observation by $R_{\rm exp} = N_{\rm exp}\langle 1/T \rangle$, taking into account the dispersion of $T$. For comparison, $N_{\rm exp}$ for Type Ia and II supernovae calculated by Woods & Loeb (1998) for the optical band is also shown in Figure 5.

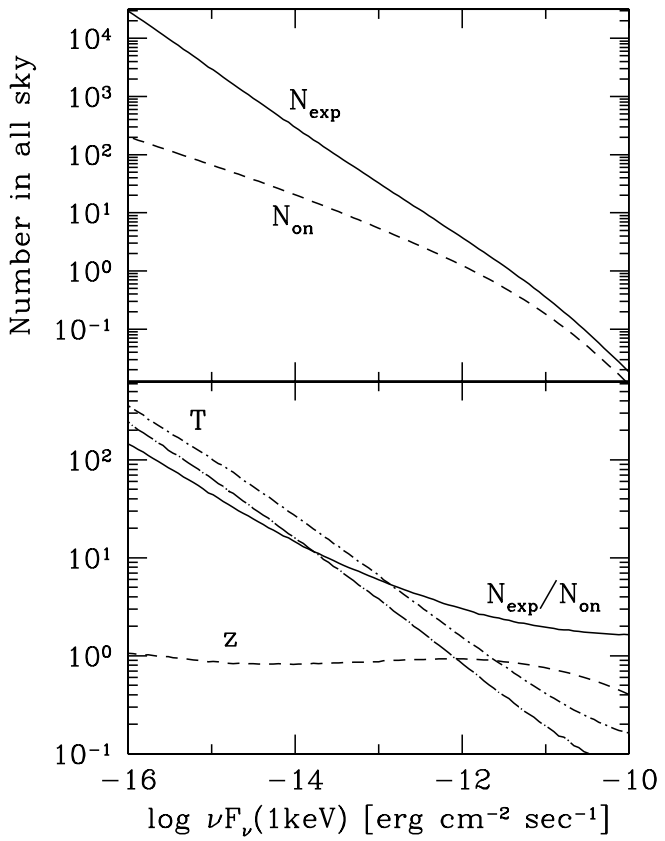


FIG. 4.—Expected number of orphan afterglows detectable by a snapshot observation per all sky, in the X-ray band (1 keV), as a function of the sensitivity limit (*top*). The solid line ($N_{\rm exp}$) is for all afterglows including orphans, while the dashed line ($N_{\rm on}$) is for on-axis afterglows that are associated with observable prompt GRBs, i.e., those with $\theta_{\rm obs} < \theta_{\rm jet}$. In the bottom panel, the ratio of $N_{\rm exp}/N_{\rm on}$, the mean values of redshift ($10^{\langle \log z \rangle}$; *dashed line*), and time duration ($T$ in days) over which the flux is above a given sensitivity are shown. For the time duration, two different means of $10^{\langle \log T \rangle}$ (*short-dash–dotted line*) and $\langle 1/T \rangle^{-1}$ (*long-dash–dotted line*) are shown.

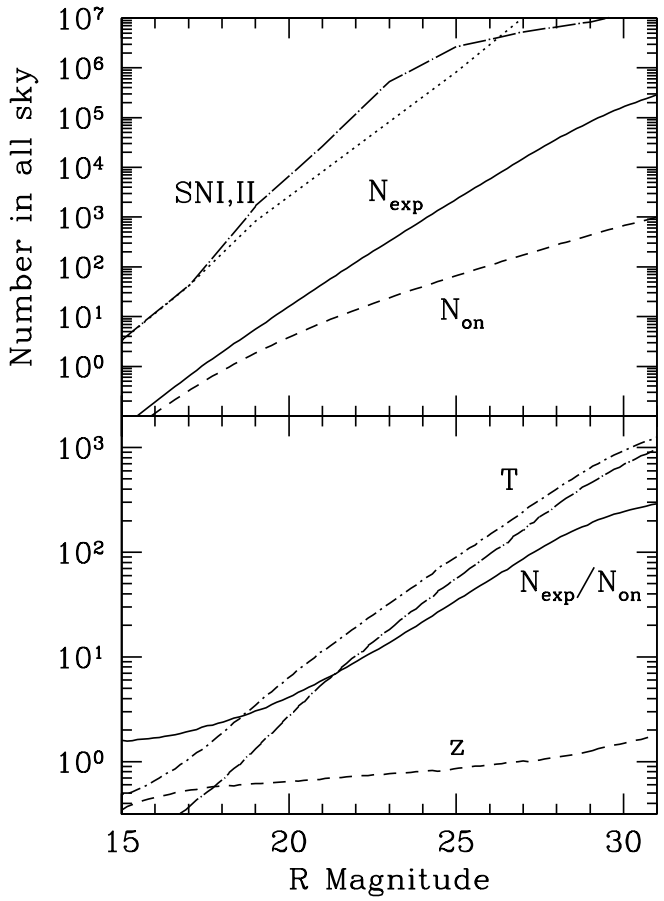


FIG. 5.—Same as Fig. 4, but for the optical ($R$) band. In addition, the expected number of supernovae of Type Ia (*dash-dotted line*) and Type II (*dotted line*) calculated by Woods & Loeb (1998) are also shown in the upper panel.

A clear trend can be seen in all wave bands; the relative beaming factor $b_{\rm rel}$ is rapidly increasing with the sensitivity limit, while the mean redshift is not. These results reflect the fact that intrinsically faint afterglows at small distances with large $\theta_{\rm obs}$ become dominant when the search sensitivity is improved. For orphan afterglow search with $b_{\rm rel} \gtrsim 10$, the required sensitivities are $\nu F_\nu \sim 10^{-14}$ to $10^{-13}$ ergs cm$^{-2}$ s$^{-1}$ and $R \sim 22$ in X-ray (1 keV) and optical bands, respectively. In the radio bands, $b_{\rm rel}$ exceeds 10 in all flux ranges shown here, while a sensitivity of $\sim$10 $\mu$Jy is necessary to increase $b_{\rm rel}$ to more than 100.

Figure 7 shows the contribution from each of the 10 GRBs to the total rate of orphan afterglows. As expected, GRB 991216 dominates in most cases, while others are important as well in the bright flux range in radio bands. It is interesting to check how the prediction is changed when the dominant GRB 991216 is removed in the sample for averaging. In the optical band, the mean rate is reduced by a factor of 2.2 and 4.5 at the search sensitivities of $R = 20$ and 25, respectively, when GRB 991216 is removed.

## 5. COMPARISON WITH PAST SEARCHES AND PROSPECTS FOR FUTURE PROJECTS

In this section we calculate the number of orphan afterglows expected in several past surveys and compare it with the reported results. We also make predictions for the num-

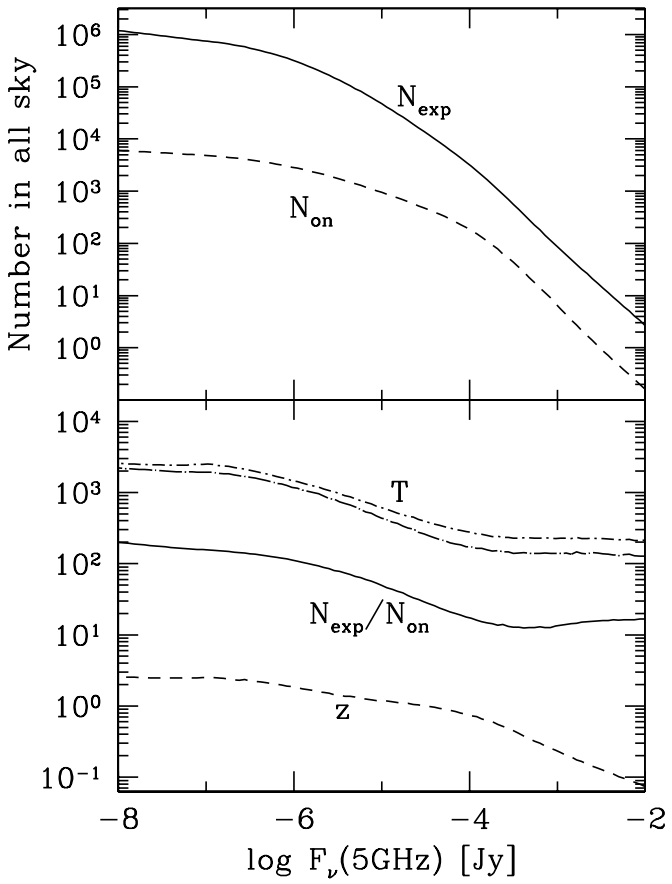


FIG. 6.—Same as Fig. 4, but for the radio (5 GHz) band

ber of orphan afterglows expected in future surveys. The summary of our results is given in Table 1.

### 5.1. *X-Ray Observations*

There are two papers that constrained the orphan afterglow rate in the X-ray band: Grindlay (1999) using the *Ariel 5* survey with a sensitivity of $\sim 10^{-10}$ ergs cm$^{-2}$ s$^{-1}$ (2–10 keV) and Greiner et al. (2000) using the *ROSAT* All-Sky Survey (RASS), which is sensitive to $\sim 10^{-12}$ ergs cm$^{-2}$ s$^{-1}$ (0.1–2.4 keV). Figure 4 shows that the relative beaming factor $b_{\rm rel}$ is about 1.6 and 3.0 for the sensitivities of *Ariel* 5 and RASS, respectively. Considering this small number, the negative result of Grindlay (1999) seems consistent with our expectation. The exposure of RASS is 76,435 deg$^2$ days, and using $\langle 1/T \rangle^{-1} \sim 0.8$ day at the RASS sensitivity, this is equivalent to a snapshot observation of $\sim$94,000 deg$^2$. Our model predicts about eight GRB afterglows for this sky coverage, among which approximately three are expected to be on-axis. Greiner et al. found 23 candidates of afterglows, but they argued that the bulk of these are likely to be nearby flaring stars. If one removes those that are suspected as flaring stars, the remaining candidates are at most $\sim$10. It is interesting that this number is very close to our expectation.

The advanced satellites such as *Chandra* or *XMM-Newton* have a typical sensitivity limit of $\sim 10^{-15}$ ergs cm$^{-2}$ s$^{-1}$ for point sources, with a field of view of $\sim 10^3$ arcmin$^2$ . At such a sensitivity, the relative beaming factor is increased to $b_{\rm rel} \sim 40$. Our model predicts that the probability of finding an orphan afterglow in the field of view of one snapshot observation is $\sim$0.02. This is apparently small, but accumulation of archive data might be useful to search and constrain orphan afterglows in the future, although discrimination from flaring stars could be a major problem again.

### 5.2. *Optical Observations*

#### 5.2.1. *Past Optical Surveys*

Schaefer (2002) searched orphan afterglows in a 264 deg$^2$ field with a sensitivity of $R = 21$. The field was examined nightly, with a total duration of 33 days. He found no afterglow candidates. By using $\langle 1/T \rangle^{-1} \sim 5.1$ days of our prediction, this observation corresponds to a snapshot observation of $264 \times 33/5.1 \sim 1500$ deg$^2$. Our model predicts that about two orphan afterglows are expected, which is $b_{\rm rel} \sim 6.2$ times higher than the case of no beaming. Therefore, our model is marginally consistent with his result. On the other hand, there is a good chance to detect orphan afterglows by continued search, and effort in this direction is encouraged.

High-redshift supernovae have been intensively searched down to $R \sim 23$ for the purpose of determination of cosmological parameters (see, e.g., Schmidt et al. 1998; Perlmutter et al. 1999). The total exposure is about a few tens of "square degree years" (Rees 1999). They are normally searching supernovae with two images separated by 1 month, which is longer than the characteristic afterglow timescale at this sensitivity ($\langle 1/T \rangle^{-1} \sim 18$ days). Therefore, the exposure is equivalent to 12 time searches in a field of a few tens of square degrees. Then we estimate that the expected detection number is about 1.6 in the past, which is $b_{\rm rel} \sim 14$ times higher than the case of no beaming. It should be noted that the past supernova searches (including that of Schaefer) are not perfectly suitable to the orphan afterglow search. Supernovae are found only in one bandpass (i.e., no color information), and spectroscopic follow-up is done only for a small number of them showing good properties for the cosmological use. It should also be noted that they sometimes find "mystery objects," which decay faster than supernovae and have no host galaxies (Schmidt et al. 1998). These objects might be orphan afterglows.

#### 5.2.2. *Sloan Digital Sky Survey*

Recently, Vanden Berk et al. (2002) reported an interesting, highly luminous transient object that might be an orphan afterglow, found in the initial 1500 deg$^2$ data of the SDSS. However, Gal-Yam et al. (2002) claimed that the host galaxy of the SDSS transient is in fact an unusual radio-loud AGN showing strong variability. Therefore, it seems very likely that the SDSS transient was an AGN flare, although the possibility of an orphan afterglow cannot be completely rejected. Here we give an estimate of the expected number of orphan afterglows in the SDSS data taken so far. Vanden Berk et al. (2002) searched transient objects by the flux difference between imaging observations and later spectroscopic observations. Although the SDSS imaging observation has a sensitivity of $r' \sim 23$, spectroscopy is not performed for all objects; the object was selected as a quasar candidate by its colors. For low-redshift quasars whose colors are similar to GRB afterglows, the sensitivity is $i' \sim 19$ (Stoughton et al. 2002). Since $R - i' \sim 0$ for typical GRB afterglows, we can consider that the sensitivity of the

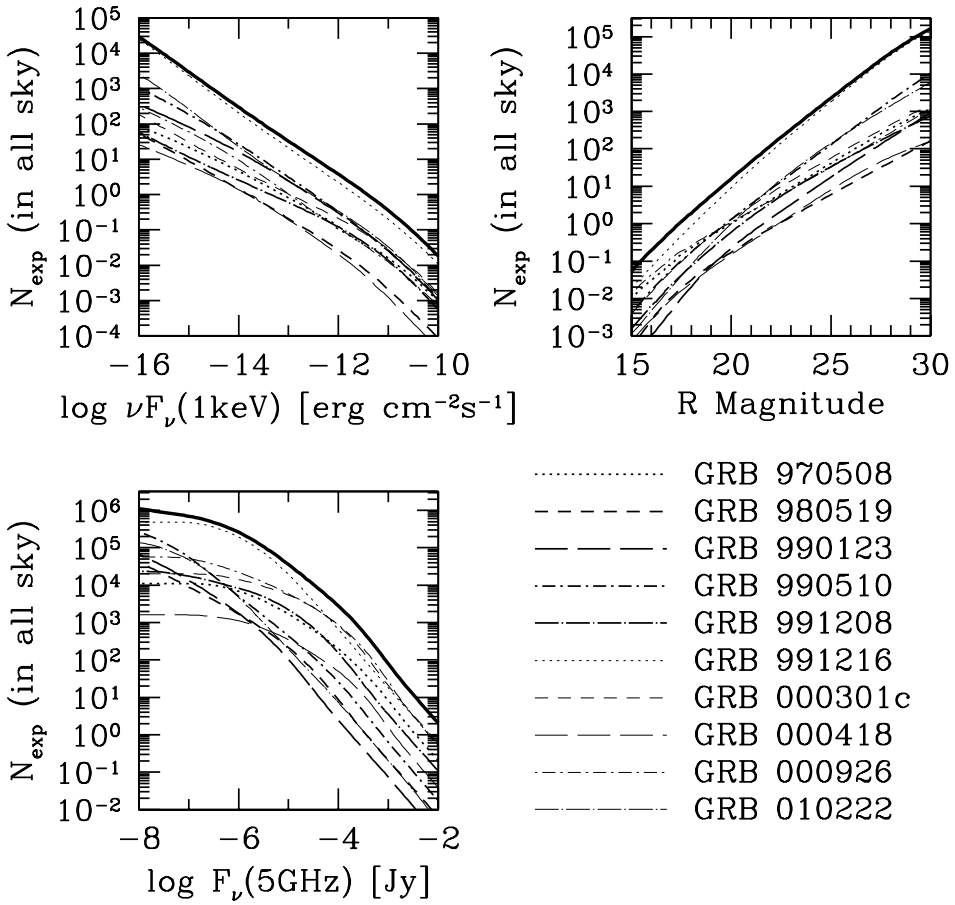


FIG. 7.—Contribution of each of the 10 GRB afterglows to the detection rate $N_{\rm exp}$ (*heavy solid line*) in the three wave bands. The line markings for the 10 afterglows are shown in the figure.

search made by Vanden Berk et al. is $R \sim 19$, with a survey area of 1500 deg$^2$. Then, we found the expected number of orphan afterglows to be $\sim$0.2, which is $b_{\rm rel} \sim 3.0$ times higher than the case of no beaming. This number is small but not extremely small compared to one detection. (Note, however, that the number becomes smaller by a factor of 10 when we apply the brightness of the SDSS transient, $R \sim 17$, as the search sensitivity.) Our model predicts the mean redshift at this sensitivity to be $10^{\langle \log z \rangle} \sim 0.6$, and the 1 $\sigma$ dispersion around this mean is $\sigma_{\log z} \sim 0.5$. Therefore, the redshift $z = 0.385$ of the host galaxy falls well in the plausible range. The characteristic timescale predicted by the model, $10^{\langle \log T \rangle} \sim 3.5$ days with $\sigma_{\log T} \sim 0.7$, is also consistent with the modest variability shown by the SDSS objects during the first two observations separated by 2 days. Therefore, it is not unreasonable even if the SDSS transient is an orphan afterglow, although the strong variability of the host galaxy indicates that the transient is much more likely an AGN flare. More statistics are obviously needed for stronger conclusions.

When the SDSS project is completed, the covering area in the northern sky will be increased to 10,000 deg$^2$. Then we expect about 1.3 orphan afterglows, which seems still small to test our model with sufficient statistics by the future data. On the other hand, the SDSS has another observing mode in the southern sky, observing a 225 deg$^2$ field repeatedly to achieve a much deeper sensitivity limit than the northern sky (see, e.g., Ivezić et al. 2000). These southern data can be used for a transient object search with a sensitivity of $R \sim 23$, which is significantly deeper than the search using spectroscopic data. The southern sky field is typically observed about four times in a year with a separation longer than 1 month. Then, at the end of the project after the planned 5 yr operation, we expect an effective survey area of $225 \times 4 \times 5 \sim 4500$ deg$^2$ (Ž. Ivezić 2002, private communication). Then we expect about 36 orphan afterglows, which is $b_{\rm rel} \sim 14$ times higher than the case of no beaming. This number suggests that we may detect a statistically meaningful number of orphan afterglows. Although spectroscopic information will not be immediately available, follow-up observations for host galaxies will give redshift information. The five-band photometry data will also help to discriminate the orphan candidates from other transient objects (Rhoads 2001). Contamination of highly variable AGNs, as in the case of the SDSS transient of Vanden Berk et al. (2002), can be removed by close examination of host galaxies in X-ray and/or radio bands and past records. (It should be noted that the host galaxy of the SDSS transient reported by Vanden Berk et al. has a strong radio emission that cannot be explained by star formation activity.) Finally, a significant part ($\sim$10%–40%) of the northern sky will also be observed more than two times because of overlaps of fields of view. The time intervals of these repetitions are not simple but depend on the survey schedule. These data can also potentially be used for orphan afterglow searches.

TABLE 1
EXPECTED NUMBER OF AFTERGLOWS IN VARIOUS SURVEYS

| Survey Name | Sensitivity | Area (deg$^2$) | $N_{\rm exp}$ | $N_{\rm on}$ | $N_{\rm exp}/N_{\rm on}$ | $10^{\langle \log z \rangle}$ | $\sigma_{\log z}$ | $10^{\langle \log T \rangle}$ | $\sigma_{\log T}$ | $\langle 1/T \rangle^{-1}$ |
|---|---|---|---|---|---|---|---|---|---|---|
| X-Ray Observation | | | | | | | | | | |
| *ROSAT*[a] | $1 \times 10^{-12}$ | $9.4 \times 10^4$ | 8.3 | 2.8 | 3.0 | 0.93 | 0.43 | 1.5 | 0.52 | 0.81 |
| Optical Observations | | | | | | | | | | |
| SDSS 1[b] | 19 | 1500 | 0.20 | 0.067 | 3.0 | 0.62 | 0.50 | 3.5 | 0.68 | 1.3 |
| SDSS 2[c] | 19 | 10000 | 1.3 | 0.45 | 3.0 | 0.62 | 0.50 | 3.5 | 0.68 | 1.3 |
| ROTSE-III | 19 | $3.9 \times 10^5$ | 53 | 18 | 3.0 | 0.62 | 0.50 | 3.5 | 0.68 | 1.3 |
| OGLE III | 20 | 5000 | 2.2 | 0.51 | 4.3 | 0.65 | 0.48 | 6.8 | 0.62 | 3.0 |
| *GAIA* | 20 | $1.7 \times 10^6$ | 720 | 170 | 4.3 | 0.65 | 0.48 | 6.8 | 0.62 | 3.0 |
| Schaefer[d] | 21 | 1500 | 1.8 | 0.29 | 6.2 | 0.69 | 0.46 | 12 | 0.58 | 5.7 |
| SDSS 3[e] | 23 | 4500 | 36 | 2.6 | 14 | 0.77 | 0.42 | 32 | 0.51 | 18 |
| Supernova[f] | 23 | 200 | 1.6 | 0.11 | 14 | 0.77 | 0.42 | 32 | 0.51 | 18 |
| DMT 1[g] | 24 | 20000 | 480 | 21 | 23 | 0.81 | 0.39 | 58 | 0.47 | 36 |
| Subaru | 26 | 5 | 0.73 | 0.013 | 55 | 0.93 | 0.32 | 150 | 0.40 | 97 |
| DMT 2[h] | 29 | 1000 | 2100 | 11 | 190 | 1.3 | 0.23 | 670 | 0.32 | 460 |
| Radio Observation | | | | | | | | | | |
| FIRST/NVSS[i] | 3.3 | 5990 | 2.0 | 0.13 | 16 | 0.13 | 0.32 | 220 | 0.39 | 140 |
| ATA | 0.16 | 5200 | 210 | 14 | 15 | 0.63 | 0.32 | 250 | 0.38 | 160 |

NOTE.—Col. (2): Sensitivity in $\nu F_\nu$ (ergs cm$^{-2}$ s$^{-1}$)$^{-1}$ at 1 keV for the X-ray band, in $R$ magnitude for the optical band, and $F_\nu$ mJy$^{-1}$ at 5 GHz in the radio band. The sensitivity is corrected based on a typical afterglow spectrum when the observation was made in a slightly different band. Col. (3): Area of a snapshot observation. When a survey is a consecutive monitoring longer than the typical afterglow timescale $T$, we converted the exposure (area-$\times$time) into an equivalent area of a snapshot observation using $\langle 1/T \rangle$. (See text for detail.) Col. (4): The total number of all GRB afterglows, including orphans, expected to be detectable by a snapshot observation with the surface is shown in the third column. Col. (5): The same as col. (4), but only for afterglows associated with prompt gamma-ray emission. Col. (6): The relative beaming factor $b_{\rm rel} \equiv N_{\rm exp}/N_{\rm on}$. Cols. (7) and (8): The mean and 1 $\sigma$ dispersion of $\log z$. Cols. (9) and (10): The mean and 1 $\sigma$ dispersion of $\log T$, where $T$ is the time duration over which afterglows are brighter than the sensitivities, in units of days. Col. (11): The mean of $T^{-1}$.

[a] The *ROSAT* All Sky Survey (Greiner et al. 2000).
[b] A search by Vanden Berk et al. 2002 using the first 1500 deg$^2$ field of the SDSS data.
[c] The same as SDSS 1, but after the completion of the SDSS project.
[d] A search made by Schaefer 2002.
[e] The number expected in the southern sky after the completion of the SDSS project.
[f] The number expected in past supernova surveys.
[g] The all-sky survey mode of the Dark Matter Telescope.
[h] The deep probe mode of the Dark Matter Telescope.
[i] The search made by Levinson et al. 2002 by using the FIRST and NVSS surveys.

#### 5.2.3. *OGLE III*

The Optical Gravitational Lensing Experiment in the third phase (OGLE III; Udalski et al. 2002) has started its operation, and during the LMC and SMC season, it will cover a 85 deg$^2$ field every night or every second night for half a year. The limiting magnitude is about $I = 19.5$ at a signal-to-noise ratio of 10 for a typical exposure of 2 minutes, corresponding to $R \sim 20$ for a typical afterglow spectrum. Using $\langle 1/T \rangle^{-1} = 3.0$ days, the total exposure of half a year is equivalent to a snapshot observation of $85 \times 180/3.0 \sim 5000$ deg$^2$. Then, about two or three orphan afterglows are expected. Since the variability timescale is only a few days at this magnitude, continuous monitoring of OGLE III with the time interval of 1 or 2 days is very useful for an afterglow search. The mean redshift is $10^{\log z} = 0.65$ with a dispersion of $\sigma_{\log z} \sim 0.5$. This means that a significant fraction of orphan afterglows detectable by OGLE III should have large redshifts of $z \gtrsim 1$. Then the brightness of $R \sim 20$ would be much brighter than any kind of supernovae, and hence, orphan afterglows and supernovae can be discriminated.

#### 5.2.4. *ROTSE-III*

The ROTSE group is considering using their ROTSE-III telescope for an orphan afterglow search, whose field of view is 3.5 deg$^2$ (Smith et al. 2002; Kehoe et al. 2002). A search planned using four instruments will cover about 1400 deg$^2$ with a limiting magnitude better than 19 each night (C. Akerlof 2002, private communication). This means that ROTSE-III has the capability of doing an orphan afterglow search equivalent to that made by SDSS (Vanden Berk et al. 2002) only in one night. If such a search is continued for a year, the effective sky coverage could reach $\sim 1400 \times 365/1.3 \sim 3.9 \times 10^5$ deg$^2$, taking into account that $\langle 1/T \rangle^{-1} = 1.3$ days at this sensitivity. Then we expect more than 50 orphan afterglows with $b_{\rm rel} \sim 3$. Since $T \lesssim 1$ day, more than one observation in a night would also be favored for sufficient time resolution.

#### 5.2.5. *Subaru/Suprime-Cam*

The Suprime-Cam of the 8.2 m Subaru Telescope is a unique facility with a field of view (FOV) of $30' \times 30'$, which is more than 100 times wider the than typical FOVs of 8 m

class telescopes or the *Hubble Space Telescope*. Therefore, this instrument is the most suitable for an orphan afterglow search at the deepest sensitivities we can achieve. A sensitivity limit of $R \sim 26$ for point sources[4] is achieved by about 10 minute exposures, and then it is possible to observe about 10 FOVs in a night with multiband photometry. A clear advantage of the deep sensitivity is that we expect a large relative beaming factor, $b_{\rm rel} \sim 50$. Then we expect about 0.4 orphan afterglows. Therefore, a detection is not extremely difficult when systematic searches are performed using several nights. We show the expected number assuming a search over a 5 deg$^2$ field in Table 1. If detected, a large value of $b_{\rm rel}$ strongly argues for the existence of many more orphan afterglows than those associated with GRBs. At this sensitivity, the timescale of afterglow variability is increased to $10^{\log T} \sim 150$ days with $\sigma_{\log T} \sim 0.4$. Therefore, a longer timescale than supernova searches may be favored.

A problem is discrimination from other transient objects. A few supernovae are typically found in one FOV of the Suprime-Cam down to $I \sim 25$ (M. Doi & N. Yasuda 2002, private communication). At this magnitude, orphan afterglows may not be sufficiently brighter than supernovae, while the SDSS transient of Vanden Berk et al. (2002) was about 100 times brighter than the brightest supernovae. Most supernovae have thermal spectra that are curved compared to those of power-law GRB afterglows. Therefore, color-color plots by multiband photometry can be used for discrimination (Rhoads 2001), although it is still uncertain whether this method can remove all supernovae including peculiar ones. Offset of optical transients from centers of galaxies, close examination of host galaxies, and past records will be useful to remove AGNs, as mentioned in the previous section.

#### 5.2.6. *GAIA*

The astrometric satellite *GAIA* will survey all the sky many times with a sensitivity of $R \sim 20$. Each location of the sky will be observed about 40 times separated by more than 1 month during the whole mission (L. Eyer 2002, private communication). Therefore, we expect about 720 orphan afterglows. While the relative beaming factor is not large ($b_{\rm rel} \sim 4.3$ at this sensitivity limit), the enormous number expected might be useful for statistical analysis of the orphan afterglow rate. Because of small $b_{\rm rel}$, the cross-check between gamma-ray observations is crucial to discriminate orphans from ordinary afterglows associated with observable GRBs. It is highly desired that a GRB satellite covering a significant part of all sky is working at the time of the *GAIA* project.

#### 5.2.7. *Dark Matter Telescope*

Even more powerful searches than that by the Subaru Suprime-Cam would become possible at the sensitivity of 8 m class telescopes by the planned Dark Matter Telescope (DMT),[5] having a 7 deg$^2$ FOV. In the planned all-sky survey mode, the DMT will cover 20,000 deg$^2$ down to 24 mag twice in the same month, in which about 500 orphan afterglows are expected with $b_{\rm rel} \sim 20$. On the other hand, the deep probe mode will cover 10 fields of 100 deg$^2$ with a sensitivity of 29 mag. Then, in principle, a few thousand orphan afterglows could be detected with $b_{\rm rel} \sim 200$, although it is not yet clear how they can be discriminated from other transient objects at such a deep sensitivity level. It should also be noted that the characteristic timescale $T$ is more than 500 days for this sensitivity, and hence a sufficiently long time interval is required for the search.

### 5.3. *Radio Observations*

Perna & Loeb (1998) used faint source counts in radio bands to constrain the orphan afterglow rate. The radio source count at 8.44 GHz is $\sim 3 \times 10^6$ in all sky for $S > 0.1$ mJy (Windhorst et al. 1993; Becker, White, & Helfand 1995). Following Perna & Loeb, we assume that about 3% of sources at this sensitivity are variable, yielding an upper bound on the number of orphan afterglows in all sky as $\lesssim 9 \times 10^4$. The power index of the radio spectrum is changing from the initial value of $\delta = -\frac{1}{3}$ (below the peak frequency) to $\delta \sim 1$ (above the peak frequency), but typically it is $\delta \sim 0.5$ at a few hundred days after the burst. Taking into account this correction from 8.44 to 5 GHz, we obtain $\sim 2 \times 10^3$ orphans expected by our model. Therefore, the current upper bound on variable radio source counts hardly constrains our model. In fact, the relative beaming factor expected at this sensitivity is $b_{\rm rel} \sim 15$, which is not greater than the maximum expected by the deepest optical search by Subaru Suprime-Cam. One might have thought that radio band is potentially the best wave band for orphan afterglow searches, since radio afterglows are visible long after the bursts and we expect a large $b_{\rm rel}$. However, in order to achieve $b_{\rm rel} \gtrsim 100$, the sensitivity must be better than $\sim$1–10 $\mu$Jy.

The difficulty in radio searches is discrimination from other variable sources such as AGNs. It is difficult to do this discrimination only in the radio band but might be possible if we utilize information in other wave bands. Intensive examination of variable objects found in the radio band with cross-checks between the radio, optical, and X-ray surveys may allow us to find an orphan afterglow in a large ($\sim$40–50) sample of variable AGNs at sensitivities of $\sim$0.1 mJy.

A unique characteristic of radio afterglow, which is different from X-ray or optical bands, is that $b_{\rm rel}$ does not decrease but stays roughly constant at $b_{\rm rel} \gtrsim 10$–20 when the search sensitivity is decreased to $F_\nu \gtrsim 1$ mJy (brightest flux region). This is coming from the properties of the radio light curves; the peak of radio light curves occurs at a relatively late time even in the on-axis case. Therefore, the radio afterglows cannot be detected at large cosmological distances even when an observer is located on the jet axis, while on-axis early afterglows in X-ray or optical bands are very bright, and they can be detected at almost all the cosmological distance scales. As can be seen in Figure 3, the peak radio flux is almost independent of $\theta_{\rm obs}$ in some dominant GRBs such as 991216, 000301c, and 000926. Therefore, $b_{\rm rel}$ converges into a finite value ($\sim$10–20) with $F_{\rm lim} \to \infty$. On the other hand, as mentioned earlier, very bright on-axis afterglows at large cosmological distances are dominant in the brightest flux range in the X-ray or optical bands, making $b_{\rm rel}$ converge to unity with $F_{\rm lim} \to \infty$. The sharp decrease of the mean redshift $\langle z \rangle$ of radio afterglow with increasing flux

[4] This estimate is not seriously affected even if an afterglow is found in a host galaxy whose luminosity is brighter than the afterglow since generally ground-based observation is limited by the sky background, and in most cases the surface brightness of galaxies is not brighter than the sky.

[5] See http://www.dmtelescope.org.

in a flux range of $F_\nu \gtrsim 1$ mJy, where $b_{\rm rel}$ is roughly constant, is also consistent with this interpretation (see Fig. 6). This effect then suggests that a relatively shallower but wide-field search is an efficient way to constrain the orphan afterglow rate in radio bands rather than deeper and narrower searches. In such a survey, low-redshift afterglows with large $T$ and $\theta_{\rm obs}$ should be dominant, which may be called GRB remnants rather than afterglows (Paczyński 2001; Ayal & Piran 2001).

Levinson et al. (2002) made a search of orphan afterglows by comparing the FIRST and NVSS surveys. Their sky coverage is 5990 deg$^2$, and they found 26 candidates of orphan afterglows, for which they argued that these are unlikely to be radio supernovae, while the possibility of radio-loud AGNs cannot be rejected. The number in 5990 deg$^2$ may be increased to $\sim$65 when corrections for incompleteness are made. Their search sensitivity is 6 mJy at 1.5 GHz, and hence we transformed this into 3.3 mJy at 5 GHz band, again assuming $\delta = 0.5$. Then we found that our expectation for this search is $N_{\rm exp} \sim 2.0$ at $b_{\rm rel} \sim 16$. Further observational inspection of these candidates is necessary, and such effort may reveal some orphan afterglows. If, instead, the majority of the candidates turn out to be orphans, it would indicate a very high orphan afterglow rate, which cannot be explained within the jet model with sharp edges.

A future project, the Allen Telescope Array (ATA), for the SETI has a sensitivity of about 0.3 mJy at 1.4 GHz (0.16 mJy at 5 GHz if $\delta = 0.5$) in 1 minute of integration time, with a pixel size of $\sim 1'$ diameter and a total beam area of $2\overset{\circ}{.}5$ diameter. At this integration time, it could cover 25% of the northern sky everyday (L. Blitz 2002, private communication; see also the ATA Web site[6]). Although the sky coverage is not much better than the FIRST/NVSS surveys utilized by Levinson et al. (2002), the better sensitivity increases the expected number of orphan afterglows greatly to $\sim$200 out to the redshift of $z \sim 0.6$ with a characteristic variability timescale of 200–300 days. Furthermore, ATA will provide radio light curves sampled everyday, which would be very useful to check whether a transient source is an orphan afterglow or not.

## 6. DISCUSSION

### 6.1. *Comparison with Previous Work*

Our result that the detection rate of orphan afterglows of collimated GRBs in optical bands could be much higher ($b_{\rm rel} \gtrsim 100$ at $R \sim 24$ for GRB 991216) than in the case of spherical GRBs seems apparently in contrast to that of Dalal et al. (2002), who showed a result that the detection rate of orphan afterglows is insensitive to the jet opening angle $\theta_{\rm jet}$ and that $b_{\rm rel}$ is constant at $\sim$3–4 for a search with a sensitivity of $R \sim 27$. We note that the result of Dalal et al. (2002) was derived assuming fixed values for the jet-break time and luminosity at the break time for an on-axis observer. In this case, the maximum viewing angle at which the afterglow can be detected ($\theta_{\rm max}$ in eq. [9]) is proportional to $\theta_{\rm jet}$, and hence the relative beaming factor $b_{\rm rel}$ does not depend on $\theta_{\rm jet}$, as can be seen from equation (9).

However, if the energy of afterglow jets does not vary much among GRBs, as suggested by Frail et al. (2001), despite a wide range of initial jet angles $\theta_{\rm jet}$ (Panaitescu & Kumar 2001), the flux at the jet-break time $F_0(\nu, t_{j,0})$ measured by an on-axis observer is strongly dependent on $\theta_{\rm jet}$, thus far from the assumption of constancy made by Dalal et al. (2002). Within the framework of relativistic jets, it can be shown that at optical frequencies $F_0(\nu, t_{j,0}) \propto \theta_{\rm jet}^{-2p}$, where $p$ is the index of the power-law electron distribution. Furthermore, after the jet-break time the slope $-\alpha_2$ of the afterglow decay is $-p$ (Rhoads 1999). Then equation (8) leads to a peak flux $F(\nu, t_p)$ for an off-axis observer that is independent of $\theta_{\rm jet}$. This conclusion can also be reached by noting that the jet dynamics after the jet-break time is independent of $\theta_{\rm jet}$ (Granot et al. 2002). As shown in § 2, for an off-axis observer, the afterglow light curve peaks after the jet-break time; therefore, the peak flux, which is determined by the jet dynamics and observer location, does not depend on the initial jet opening. That $F(\nu, t_p)$ is independent of $\theta_{\rm jet}$ implies that $\theta_{\rm max}$ does not depend on $\theta_{\rm jet}$, and the original expectation $b_{\rm rel} \propto (\theta_{\rm max}/\theta_{\rm jet})^2 \propto \theta_{\rm jet}^{-2}$ is restored.

The above result regarding the constancy of $F(\nu, t_p)$ is illustrated in Figure 8, where we show the light curves of optical afterglows with various values of $\theta_{\rm jet}$ for an observer located at $\theta_{\rm obs} = 20°$. Here we used a fixed set of typical afterglow model parameters (other than $\theta_{\rm jet}$): $E_{\rm jet} = 3 \times 10^{50}$ ergs, $n_{\rm ext} = 1$ cm$^{-3}$, $\epsilon_e = 0.05$, $\epsilon_B = 3 \times 10^{-3}$, and $p = 2$. The peak flux hardly changes with $\theta_{\rm jet}$ at $\theta_{\rm jet} \lesssim 5°$. Figure 9 shows the beaming factor $b_{\rm rel}$ as a function of $\theta_{\rm jet}$ for various sensitivities. Note that $b_{\rm rel}$ becomes larger for more collimated GRBs, asymptotically reaching the expected relation $b_{\rm rel} \propto \theta_{\rm jet}^{-2}$ when $\theta_{\rm jet} \to 0$. Thus, orphan afterglow searches could give useful information on the GRB collimation.

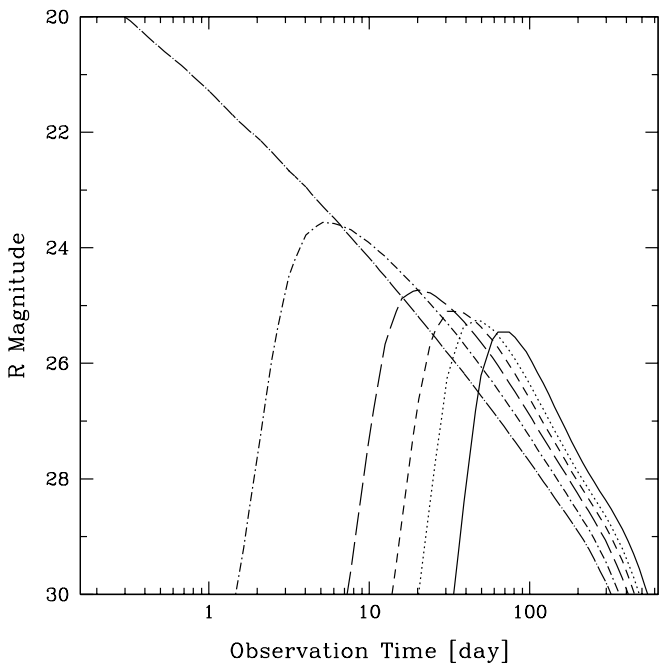


FIG. 8.—Optical light curves of orphan afterglows, for a fixed viewing angle $\theta_{\rm obs} = 20°$, but various jet opening angles, $\theta_{\rm jet}$. The solid, dotted, short- and long-dashed, and short- and long-dash–dotted lines are for $\theta_{\rm jet} = 1°$, $2°$, $3°$, $5°$, $10°$, and $20°$, respectively. The redshift is assumed to be 1. Other parameters of the afterglow model are $E_{\rm jet} = 3 \times 10^{50}$ ergs, $n_{\rm ex} = 1$ cm$^{-3}$, $\epsilon_e = 0.05$, $\epsilon_B = 3 \times 10^{-3}$, and $p = 2$.

[6] Available at http://www.seti-inst.edu/science/ata.html.

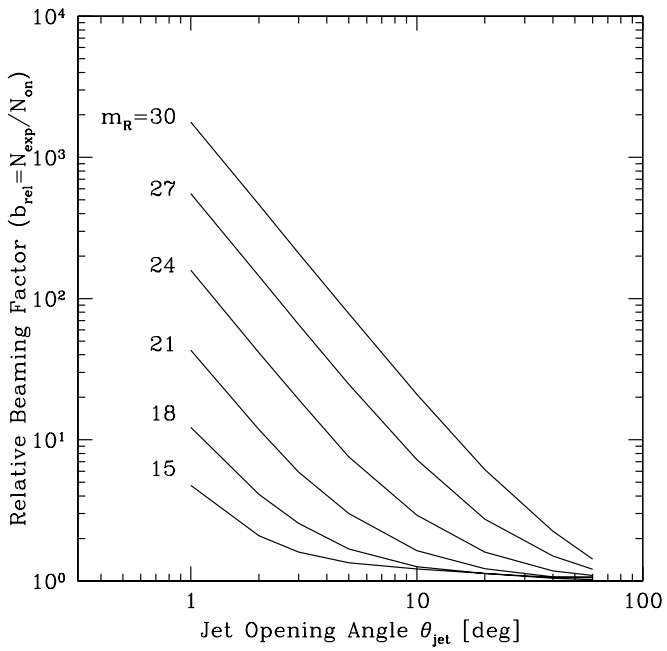


FIG. 9.—$\theta_{\rm jet}$ dependence of the relative beaming factor $b_{\rm rel}$, i.e., the ratio of rate for all afterglows, including orphans, to those associated with prompt GRBs. Different curves correspond to different search sensitivities in optical band, as indicated in the figure. Other parameters of the afterglow model are $E_{\rm jet} = 3 \times 10^{50}$ ergs, $n_{\rm ex} = 1$ cm$^{-3}$, $\epsilon_e = 0.05$, $\epsilon_B = 3 \times 10^{-3}$, and $p = 2$.

### 6.2. *Uniform versus Universal Jet Profile*

In this work we have assumed a conical jet with a sharp edge, a uniform energy per solid angle within the jet opening, and no energy outside (the *uniform jet model*). Such a model is appropriate if the angular distribution of the energy has a characteristic angular scale and decreases rapidly beyond it, e.g., an exponential profile $\propto \exp(-\theta/\theta_{\rm jet})$. In this model, the observed anticorrelation between isotropic equivalent luminosity and jet-break time can arise if jets have roughly the same energy but different opening angles $\theta_{\rm jet}$ among bursts (Frail et al. 2001). However, if the energy per solid angle has a large variation but no characteristic scale (e.g., a power-law distribution), a completely different picture is possible. Some recent papers proposed that the observed luminosity–break time anticorrelation can be explained by a *universal jet* with a nonuniform profile, observed at different viewing angles (Rossi, Lazzati, & Ress 2002; Salmonson & Galama 2002; Zhang & Mészáros 2002), which can be an alternative to the uniform jet model. In such a model, the angular distribution of jet energy per unit solid angle should be a power law $(d\mathscr{E}/d\Omega) \propto \theta^{-2}$ to reproduce the above-mentioned correlation.

It is not straightforward to predict how the orphan afterglow rate is changed when such a picture is adopted rather than the uniform jet model. If we have an ideal gamma-ray detector that can detect all GRBs everywhere in the universe, then we expect that $b_{\rm rel}$ cannot be much greater than unity in the universal jet picture because of the following reason. We expect orphan afterglows only when viewing angles larger than an angle $\theta_\gamma$ corresponding to either the maximum angular spread of the jet or the angle at which small energy per solid angle and/or the Lorentz factor yield a barely detectable gamma-ray emission. The orphan afterglow rate should then be close to that predicted by our model for a jet of opening angle $\theta_\gamma$. An estimate of $\theta_\gamma$ can be obtained as follows. The isotropic equivalent gamma-ray energies calculated by Bloom, Frail, & Sari (2001) for bursts with known redshifts span 2–3 orders of magnitude. If the GRB output is mainly determined by the jet energy per solid angle toward the observer, then the above distribution $(d\mathscr{E}/d\Omega) \propto \theta^{-2}$ implies that the dimmest GRB jets are seen at an angle at least 10 times larger than that for the brightest jets. The latter angle should be around the smallest jet opening angle of 2° found by Panaitescu & Kumar (2002) by modeling the broadband emission of 10 afterglows using the uniform jet model,[7] leading to $\theta_\gamma \gtrsim 20°$. Since the relative beaming factor decreases with the jet opening angle, as shown in Figure 9, we expect that for the universal structured jet model, $b_{\rm rel} \sim$ a few for the reasonable search sensitivities of $R \lesssim 27$. On the other hand, as we have shown in Figure 5, it rapidly increases to $b_{\rm rel} \sim 50$ with the sensitivity to $R \sim 26$ in the uniform jet model.

However, we may have orphan afterglows due to an insufficient gamma-ray sensitivity. Since the gamma-ray luminosity per unit solid angle rapidly increases with decreasing $\theta_{\rm obs}$ in the universal jet model, the detection of GRBs at large distances might be biased toward those with small $\theta_{\rm obs}$. If this is the case, we expect a much higher true GRB rate, and large $b_{\rm rel}$ might be possible also in the universal jet picture. A test for this case is to see an anticorrelation between $z$ and $\theta_{\rm obs}$ and confirm or reject the $\theta_{\rm obs}$ distribution obeying $N(< \theta_{\rm obs}) \propto (1 - \cos\theta_{\rm obs})/2$, as predicted by the universal jet model, for a complete sample of GRBs within a redshift range. The distribution of $\theta_{\rm obs}$ can be observationally inferred from either the luminosity function of GRBs with $z$ measurements or the jet-break time obtained by afterglow light-curve fitting. However, the present sample of GRBs with known redshifts is too small, and we must await future observations.

Another test possible by orphan afterglow observation is to examine the early behavior of orphan afterglow light curves. For $\theta_{\rm obs} > \theta_{\rm jet}$ in the uniform jet model, we always expect no afterglow flux at the earliest stage, and the afterglow flux should show gradual increase until the peak flux time, $t_p$, given in § 2. When $b_{\rm rel} \gg 1$, the orphan afterglow events should be dominated by such cases, and hence we expect that the majority of orphan afterglows should show a slow rise at the beginning. On the other hand, the X-ray and optical emission should start immediately after the prompt burst when $\theta_{\rm obs} < \theta_\gamma$ in the universal jet picture since there are ejecta moving toward the observer. The initial slow rise of light curves is possible only when $\theta_{\rm obs} > \theta_\gamma$, but such events should be relatively rare because of the large $\theta_\gamma$ inferred from observations and low absolute luminosity for the large $\theta_{\rm obs}$ cases. The detection of such an early rise of light curves may not be easy even in the case of the uniform jet model because the rising timescale is still smaller than the overall variability timescale $T$ as can be seen in Figures 1 and 2. If detected, however, it would argue for the uniform jet picture.

[7] Rossi et al. (2002) have shown that the jet initial opening inferred in the uniform jet model is in fact the observer's angular offset relative to the jet axis in the universal jet model.

### 6.3. *Caveats of Our Predictions*

Here we describe several caveats of our prediction that should be kept in mind when one compares it to observed data.

It is theoretically conceivable that the GRB central engine ejects not only the ultrarelativistic outflow that is responsible for GRBs but also less relativistic matter with comparable total energy. Prompt gamma-ray emission may be very dim or completely absent from such less relativistic components of ejecta, while the afterglow emission similar to those associated with GRBs might be possible. Even if the ultrarelativistic component may be strongly collimated to produce beamed GRBs, a more isotropic, less relativistic component could be associated with most of GRBs. It is also possible that there is much larger number of events of dirty fireball or failed GRBs without prompt gamma-ray emission to any direction than that of observed GRBs. The brightest class of core-collapse supernovae, called hypernovae (Iwamoto et al. 2000; Nakamura et al. 2001; Mazzali et al. 2002), might also be failed GRBs. In either case, the orphan afterglow rate can be increased significantly from our prediction. Even if an orphan afterglow is discovered, it is not an easy task to discriminate such another component of ejecta or failed GRBs from the pure effect of GRB jet collimation (Huang et al. 2002).

One possible way of discrimination between an orphan afterglow due solely to the viewing geometry from one due to a dirty fireball is provided by the afterglow decay rate. In the former case, the jet collimation should yield a decay slope $\alpha \sim -2$, while a less collimated component or a failed GRB is expected to yield $\alpha \sim -1$. The slower rise of the light curves of off-axis, collimated jets is also useful, as discussed in the previous subsection (see also Huang et al. 2002). Stronger linear polarization is also expected for off-axis, collimated jets (Sari 1999; Ghisellini & Lazzati 1999; Granot et al. 2002). Finally, the wavelength and sensitivity dependence of $b_{\rm rel}$ might be able to discriminate the above possibilities. The signature of off-axis afterglows would be the continuous increase of $b_{\rm rel}$ with the search sensitivity, although this trend might be mimicked by failed GRBs if their event rate is continuously increasing with decreasing energy output to the dirty component. The constraint of $b_{\rm rel} \lesssim$ several by the past X-ray searches already indicates that the event rate of failed GRBs producing X-rays cannot be much higher than that of successful GRBs. On the other hand, the so-called X-ray–rich GRBs might be a population between the failed and ordinary GRBs (see, e.g., Kippen et al. 2002).

We have assumed that the sky coverage of the gamma-ray emission is that corresponding to the jet opening angle obtained from afterglow modeling. However, this is not necessarily warranted. The causally connected angular scale during the prompt GRB phase is only $\theta \sim \Gamma^{-1}$, which should be much smaller than the jet opening angle $\theta_{\rm jet}$ (Kumar & Piran 2000). Then it is possible that the jet outflow, and thus its gamma-ray emission, is inhomogeneous on an angular scale much smaller than $\theta_{\rm jet}$, while the afterglow emission arising later in the jet evolution is more homogeneous. In this case the GRB rate is significantly underestimated since there could be a number of undetected GRBs due to some low-energy patches moving toward the observer, even if the observer is located within the jet opening angle.

We have also assumed that the 10 GRB afterglows used here are representative for all varieties of GRB afterglows. Although X-ray afterglows were observed for the majority of GRBs, optical afterglows were found for less than half of GRBs. Some afterglows were missed because of late follow-up observations, but there were also unusually dim optical afterglows (Fynbo et al. 2001; Lazzati, Covino, & Ghisellini 2002). Several explanations can be considered including dust extinction and very large redshift. Recent studies of high-redshift galaxies suggest that about half of stars are formed in very dusty galaxies, the fraction being much larger at high redshift than in the local universe (see, e.g., Totani & Takeuchi 2002; Ramirez-Ruiz, Trentham, & Blain 2002). The sample of the 10 afterglows used here is clearly biased toward afterglows occurring in less dusty galaxies. Then our estimate of the optical orphan afterglow rate may be overestimated by a factor of about 2. When a GRB occurs in a molecular cloud or high-density region with a significant amount of dust, the dust along the direction of the jet might be destroyed by a strong optical-UV flash (Waxman & Draine 2000) or early X-radiation (Fruchter, Krolik, & Rhoads 2001), making optical afterglows visible for on-axis observers. However, this effect should be small for off-axis observers because the off-axis X-ray afterglow flux is much weaker when the light curve peaks. This phenomenon may effectively reduce the observed relative beaming factor $b_{\rm rel}$. Finally, it should be noted that the prediction for radio orphan afterglows is not affected by dust extinction.

## 7. CONCLUSIONS

We presented a quantitative prediction for the detection rate of orphan GRB afterglows, based on one of the latest afterglow models that has been tested with a number of observed afterglows. We found that the orphan afterglow rate sensitively depends on afterglow model parameters and that a fairly large $b_{\rm rel}$ ($\gtrsim 100$) is possible for some types of GRBs by an optical search with reasonable depth ($R \gtrsim 24$). We derived our best-guess prediction of the orphan afterglow rate by taking a weighted mean of the 10 sets of afterglow parameters that fitted to 10 well-observed afterglows. Although there are a number of effects or caveats that could significantly change our predictions, the prediction will be useful as "a baseline model" when we interpret the results of past and future surveys for extragalactic transient objects.

Our prediction is consistent with all the past surveys in X-ray, optical, and radio wave bands. Greiner et al. (2000) reported that there are about 10 possible candidates of orphan afterglows, which is interestingly very close to our expectation. Although the SDSS transient reported by Vanden Berk et al. (2002) is very likely to be a radio-loud AGN, their search has already reached a meaningful sensitivity since our expectation is about 0.2 afterglows for this search. A recent search by Levinson et al. (2002) found about 30 candidate radio afterglows by comparing the FIRST and NVSS surveys, while our model expects about two orphans.

Detection of orphan afterglows seems not extremely difficult in future surveys. Accumulation of data of advanced X-ray satellites such as *Chandra* and *XMM-Newton* might detect orphan afterglows whose rate is enhanced by a relative beaming factor of $b_{\rm rel} \sim 40$ compared to that for GRB-associated afterglows. The OGLE III and ROTSE-III proj-

ects could detect a few and a few tens of orphan afterglows with $b_{\rm rel} \sim 3$–4 in half a year at $R \sim 20$ and 19, respectively, providing nightly light curves. The southern SDSS observation ($R \sim 23$) could detect about 40 orphan afterglows with $b_{\rm rel} \sim 14$ during five years of operation. Further deep optical surveys by Subaru Suprime-Cam ($R \sim 26$) might detect an orphan afterglow with $b_{\rm rel} \sim 50$. In the more distant future, *GAIA* could detect ~900 afterglows down to $R \sim 20$, and DMT could detect 500 and 2000 orphans at $R = 24$ and 29, respectively.

ATA would detect about 200 orphans with $b_{\rm rel} \sim 15$ at ~0.3 mJy (1.4 GHz) in the radio band. Further effort for these searches is encouraged in the near future. Finally, we should make a point that a future GRB mission monitoring a significant part of all sky, like BATSE, is desired to check whether a candidate orphan afterglow is really an "orphan." It is crucial especially for shallow searches of orphan afterglows with small relative beaming factor.

We would like to thank C. Akerlof, L. Blitz, M. Doi, L. Eyer, Ž. Ivezić, D. Lazzati, T. Mihara, T. Murakami, B. Paczyński, E. Ramirez-Ruiz, D. Vanden Berk, and N. Yasuda for many useful comments and discussions. T. T. has been financially supported by the JSPS Postdoctoral Fellowship for Research Abroad. A. P. acknowledges the support received from the Lyman Stizer, Jr. Fellowship.

## REFERENCES

Ayal, S., & Piran, T. 2001, ApJ, 555, 23
Becker, R. H., White, R. L., & Helfand, D. J. 1995, ApJ, 450, 559
Bloom, S., Frail, D., & Sari, R. 2001, AJ, 121, 2879
Dalal, N., Griest, K., & Pruet, J. 2002, ApJ, 564, 209
Frail, D. A., et al. 2001, ApJ, 562, L55
Fruchter, A., Krolik, J. H., & Rhoads, J. E. 2001, ApJ, 563, 597
Fynbo, J. U., et al. 2001, A&A, 369, 373
Gal-Yam, A., Ofek, E. O., Filippenko, A. V., Chornock, R., & Li, W. 2002, PASP, 114, 587
Ghisellini, G., & Lazzati, D. 1999, MNRAS, 309, L7
Granot, J., Panaitescu, A., Kumar, P., & Woosley, S. 2002, ApJ, 570, L61
Greiner, J., Hartmann, D. H., Voges, W., Boller, T., Schwarz, R., & Zharikov, S. V. 2000, A&A, 353, 998
Grindlay, J. E. 1999, ApJ, 510, 710
Huang, Y. F., Dai, Z. G., & Lu, T. 2002, MNRAS, 332, 735
Ivezić, Ž., et al. 2000, AJ, 120, 963
Iwamoto, K., et al. 2000, ApJ, 534, 660
Kehoe, R., et al. 2002, ApJ, submitted (astro-ph/0205008)
Kippen, R. M., Woods, P. M., Heise, J., in't Zand, J. J. M., Briggs, M. S., & Preece, R. D. 2002, in Gamma-Ray Burst and Afterglow Astronomy 2001, ed. G. Ricker et al. (Woodbury: AIP), in press
Kulkarni, S. R., et al. 1999, Nature, 398, 389
Kumar, P., & Panaitescu, A. 2000, ApJ, 541, L9
Kumar, P., & Piran, T. 2000, ApJ, 535, 152
Lazzati, D., Covino, S., & Ghisellini, G. 2002, MNRAS, 330, 583
Levinson, A., Ofek, E., Waxman, E., & Gal-Yam, A. 2002, preprint (astro-ph/0203262)
Mazzali, P. A., et al. 2002, ApJ, 572, L61
Mészáros, P., & Rees, M. 1997, ApJ, 476, 232
Nakamura, T., Mazzali, P. A., Nomoto, K., & Iwamoto, K. 2001, ApJ, 550, 991
Paczyński, B. 2001, Acta Astron., 51, 1
Panaitescu, A., & Kumar, P. 2000, ApJ, 543, 66
Panaitescu, A., & Kumar, P. 2001, ApJ, 560, L49
———. 2002, ApJ, 571, 779
Perlmutter, S., et al. 1999, ApJ, 517, 565
Perna, R., & Loeb, A. 1998, ApJ, 509, L85
Ramirez-Ruiz, E., Trentham, N., & Blain, A. W. 2002, MNRAS, 329, 465
Rees, M. J. 1999, A&AS, 138, 491
Rhoads, J. E. 1997, ApJ, 487, L1
———. 1999, ApJ, 525, 737
———. 2001, ApJ, 557, 943
Rossi, E., Lazzati, D., & Rees, M. J. 2002, MNRAS, 332, 945
Salmonson, J. D., & Galama, T. J. 2002, ApJ, 569, 682
Sari, R. 1999, ApJ, 524, L43
Schaefer, B. E. 2002, in Gamma-Ray Burst and Afterglow Astronomy 2001, ed. G. Ricker et al. (Woodbury: AIP), in press
Schmidt, B. P., et al. 1998, ApJ, 507, 46
Schmidt, M. 1999, ApJ, 523, L117
Smith, D. A., et al. 2002, Gamma-Ray Burst and Afterglow Astronomy 2001, ed. G. Ricker et al. (Woodbury: AIP), in press
Stoughton, C., et al. 2002, AJ, 123, 485
Totani, T. 1997, ApJ, 486, L71
———. 1999, ApJ, 511, 41
Totani, T., & Takeuchi, T. T. 2002, ApJ, 570, 470
Udalski, A., et al. 2002, Acta Astron., 52, 1
Vanden Berk, D. E., et al. 2002, ApJ, 576, 673
Waxman, E., & Draine, B. T. 2000, ApJ, 537, 796
Wijers, R. A. M. J., Bloom, J. S., Bagla, J. S., & Natarajan, P. 1998, MNRAS, 294, L13
Windhorst, R. A., Fomalont, E. B., Partridge, R. B., & Lowenthal, J. D. 1993, ApJ, 405, 498
Woods, E., & Loeb, A. 1998, ApJ, 508, 760
Zhang, B., & Mészáros, P. 2002, ApJ, 571, 876